Available online at www.sciencedirect.com

SciVerse ScienceDirect

Solar Energy 86 (2012) 1750–1760

SOLAR ENERGY

www.elsevier.com/locate/solener

Photovoltaic dynamic MPPT on a moving vehicle

Shih-Hung Ko [a,*], Ru-Min Chao [a,b]

[a] Department of Systems and Naval Mechatronics Engineering, National Cheng Kung University, Tainan 701, Taiwan, ROC
[b] Research Center for Energy Technology and Strategy, National Cheng Kung University, Tainan 701, Taiwan, ROC

Received 8 December 2011; received in revised form 20 March 2012; accepted 22 March 2012
Available online 23 April 2012

Communicated by: Associate Editor Nicola Romeo

Abstract

In addition to the conversion efficiency of a photovoltaic panel, the maximum power point tracking (MPPT) method also plays a central role to harvest most energy out of sun. The MPPT unit on a moving vehicle must keep tracking accuracy high in order to compensate rapid change of insolation due to dynamic motion of the vehicle. In this paper, some problems of a PV system associated with a moving vehicle are addressed, and a modified quadratic maximization MPPT algorithm is proposed. Theoretical PV performance is linked to the experimental test followed by the Sandia dynamic test protocol to verify the proposed MPPT method. Finally, experimental result on a model ship is discussed.

Keywords: Maximum power point tracking (MPPT); Quadratic maximization; Photovoltaic (PV); Dynamic tracking

1. Introduction

Photovoltaic (PV) generation, as one of the most essential renewable energy sources, exhibits numerous merits such as cleanness, low maintenance, and no noise. Several applications employing this technology have been developed, such as satellite power systems, solar power generation, solar battery charging stations, and solar vehicles (for instance, car, ships, and airplanes). When a PV MPPT system is installed in a vehicle, some obstacles must be overcome to extract the most power from the PV panels.

Generally, the equivalent circuit of a solar cell can be represented by a single-diode model (Phang et al., 1984). The single-diode model includes four components: a photocurrent source, a diode parallel to the source, a series resistor and a shunt resistor. According to this model, the relation between voltage and current of a solar cell can be expressed as (Xiao et al., 2004; Bose et al., 1985)

$$I_{PV} = I_{ph} - \frac{V_{PV} + I_{PV}R_s}{R_{sh}} - I_{sat}\left[e^{\frac{q(V_{PV}+I_{PV}R_s)}{AkT}} - 1\right] \quad (1)$$

$$I_{ph} = [I_{SC} + K_I(T - T_r)]\frac{\lambda}{1000} \quad (2)$$

$$I_{sat} = I_{sat,r}\left(\frac{T}{T_r}\right)^3 \exp\left[\frac{qE_{GO}}{KA}\left(\frac{1}{T_r} - \frac{1}{T}\right)\right] \quad (3)$$

On the basis of (1)–(3), the current–voltage (I–V) curve of a photovoltaic panel, constructed by serial and parallel connection of solar cell, under different solar radiation and cell temperature can be obtained. For example, the current–voltage and power–voltage curves of a CHIMEI CSSS-90A PV module are plotted in Fig. 1 and its specifications are tabulated in Table 1. The short circuit current temperature coefficient K_I is 0.00128 A/K, E_{GO}, band gap is 1.7 eV, and the ideality factor A is 1.8. As shown in Fig. 1, under specific irradiance and temperature each curve has a maximum power point (MPP), at which the PV module gives the highest power output. Clearly, the

* Corresponding author. Tel.: +886 6 2747018x229; fax: +886 6 2747019.
E-mail addresses: yalato_ko@hotmail.com (S.-H. Ko), rmchao@mail.ncku.edu.tw (R.-M. Chao).

0038-092X/$ - see front matter © 2012 Elsevier Ltd. All rights reserved.
http://dx.doi.org/10.1016/j.solener.2012.03.013

Nomenclature

A	ideality factor, dimensionless.
D	duty ratio of pulse width modulation signal.
E_{GO}	band gap, electron V.
I_{ph}	photocurrent, A.
I_{PV}	cell output current, A.
I_{sat}	saturation current, A.
$I_{sat,r}$	saturation current at reference temperature, A.
I_{SC}	short circuit current at reference temperature, A.
k	Boltzmann constant, $k = 1.38 \times 10^{-23}$ J/K.
K_I	short circuit current temperature coefficient, A/K.
q	elementary charge, $q = 1.60 \times 10^{-19}$ C.
R_{DS}	on-state resistance of MOSFET, Ω.
R_L	direct current resistance of a inductor, Ω.
R_s	series resistance, Ω.
T	cell absolute temperature, K.
T_r	reference absolute temperature, K.
V_{FW}	diode forward voltage drop, V.
V_{PV}	cell output voltage, V.
α	reducing coefficient #1 used in modified quadratic maximization method.
β	reducing coefficient #2 used in modified quadratic maximization method.
ε	enlarging coefficient #1 used in modified quadratic maximization method.
γ	enlarging coefficient #2 used in modified quadratic maximization method.
λ	insolation level, W/m^2.

PV module has a maximum power point at certain environment condition and the MPP also changes with the irradiance and the temperature change. It is therefore necessary to track continuously the MPP in order to maximize the power output on a dynamic operating condition, caused either by environment or motion, or both.

To harvest the maximum electricity from the solar cell, the power converter of the PV system has a function called MPPT (maximum power point tracking). For example, a typical PV system consists of a PV array, a DC/DC converter, loads, and a MPPT controller. The DC/DC converter uses the MPPT controller to increase the efficiency of the PV system. By matching the impedance of the PV array with that of the converter by controlling the duty cycle of the internal switch, one can acquire maximum power from the PV array. Thus a well-designed MPPT algorithm must be able to locate the accurate maximum power point under various atmospheric conditions.

There are two system methodologies generally used for the MPPT purpose. Firstly, a voltage regulator is required to regulate the voltage out of the PV array, and the MPPT is performed to locate the optimal PV operating voltage (Xiao et al., 2007). Secondly, the controller directly locates the optimal operating duty cycle of the internal switch in the DC/DC converter. Since there is no PV voltage regulator in the second design, the system configuration is simpler and cheaper, and is commonly used in most PV system. In this paper, the design of PV system follows the second one.

In recent years, a large number of techniques have been proposed for tracking the maximum power point (Patel and Agarwal, 2009; Liu et al., 2008; Petrone et al., 2008; Esram and Chapman, 2007; Jain and Agarwal, 2007; Salas et al., 2006; Koutroulis et al., 2001). Among them perturb and observe (P&O), hill climbing (HC) and incremental conductance (INC) are three most widely discussed MPPT methods. The P&O method perturbs the operating voltage of a PV array, then observes the extracted power to modify the perturb direction (Femia et al., 2005). The HC method is similar to P&O, but it perturbs the operating duty cycle of power converter and is more attractive due to its simplified control structure. The INC method is based on the fact that the slope of the PV array power versus voltage curve is zero at the MPP, and improves the tracking accuracy and dynamic performance under rapidly varying conditions (Hussein et al., 1995).

Quadratic Maximization (QM) method (Chao et al., 2009; Pai and Chao, 2010) approximates the PV power versus duty cycle characteristic by a quadratic curve function. The operating mechanism is illustrated in Fig. 2, where the solid line represents the power versus duty cycle curve of a PV array. In general, by applying the three operating duty point D_1, D_2, and D_3 to the PV system, the corresponding PV array power output P_1, P_2, and P_3 can be measured. A quadratic curve (the dash line) then can be calculated to find the approximated MPP. If necessary, a duty shifting strategy is required to ensure the convergence of the method. This method has been proven effectively working under rapid insolation change conditions. No further perturbation is required once it reaches its MPP, a different aspect from the P&O method.

There is less information regarding to MPPT performance report in a moving vehicle. When tested in our early work, there are some problems remain when applying the QM method to a moving vehicle. Since the transient insolation condition varies with the vehicle's dynamic response of rolling, yawing and pitching, it also establishes a rigorous operation condition for any MPPT algorithm to be tested. Unnecessary tracking step or system perturbation can reduce the PV system short term performance and long term electric component reliability. When previous QM method is applied to a moving solar auxiliary powered boat, the efficiency of the PV system will be reduced due

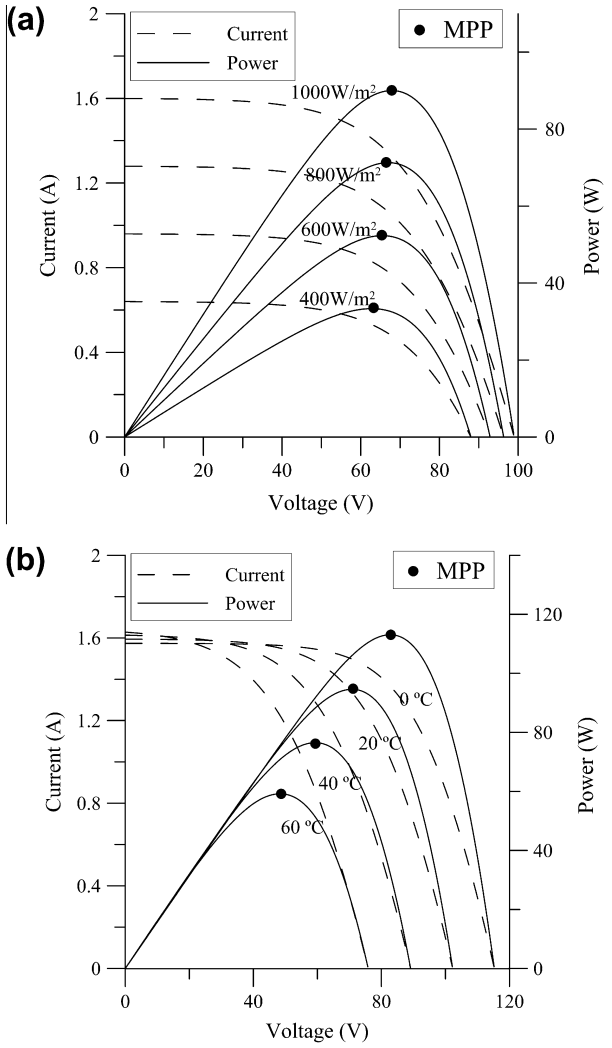

Fig. 1. I–V and P–V characteristics of thin film PV module, CSSS90A: (a) light intensity characteristic at 25 °C; (b) temperature characteristic at 1000 W/m^2.

Table 1
Specification of photovoltaic module CSSS-90A.

Model	CSSS-90A
Photovoltaic cells	Amorphous thin-film
Manufacturer	Chi mei energy
Voltage at MPP @ STC	71.4 V
Current at MPP @ STC	1.26 A
Short-circuit current @ STC	1.60 A
Open-circuit voltage @ STC	99 V

to the over perturbing of the operating points. To solve this problem, this paper analyzes the operating conditions on a moving vehicle and introduces a modified QM method. The proposed method is also benchmark tested according to Sandia dynamic test protocol for solar application. In Section 2 some characteristics of a PV system on a moving vehicle are analyzed, and some limitations of previous QM method under this operating condition are also discussed.

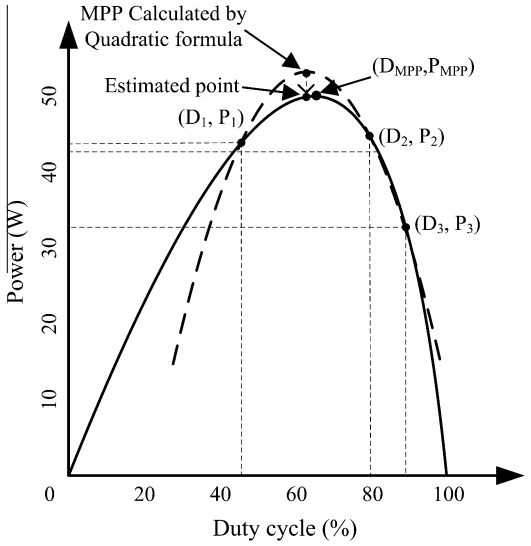

Fig. 2. Illustration of quadratic maximization MPPT mechanism.

In Section 3, a modified QM algorithm is proposed. The PSIM software performs the PV characteristic simulation and the result is implemented into LabVIEW as the PV source. The benchmark test among the P&O method, previous QM and modified QM algorithms under LabVIEW are tested and reported. In Section 4, experiments following the Sandia dynamic testing protocol of solar application, and test report on a model ship are also given. In Section 5, conclusions end this paper.

2. Previous QM MPPT method used on a moving vehicle

The PV system on a moving vehicle is a standalone PV application. The PV array and battery are connected through a power converter, and a MPPT controller can control the operating voltage of a PV array and the battery charging current. In general, a battery bank is connected to the PV system for providing electric power and energy storage. The terminal voltage V_{BAT} of the battery does not change in a short period of time and can be treated as a constant during analyzing. For a PV system using buck converter, as shown in Fig. 3, a DC model can be derived and the relation between V_{PV} and operating duty cycle is given by Erickson and Maksimović (2001)

$$V_{PV} = \frac{V_{BAT}}{D} + \frac{1-D}{D} V_{FW} + \frac{R_{DS}}{D} I_{PV} + \frac{R_L}{D^2} I_{PV} \tag{4}$$

where the relation between V_{PV} and I_{PV} in (4) is described in (1)–(3).

Considering the operating conditions of a PV system under different irradiation and temperature with buck converter, the power versus duty cycle characteristic curves can be derived from (1)–(4) and simulated by PSIM software. Simulation parameters are shown in Tables 1 and 2, and the battery terminal voltage is 24 V. As shown in Fig. 4, the D_{MPP}, duty cycle at MPP is obviously affected by operating temperature of a PV array on the moving vehicle.

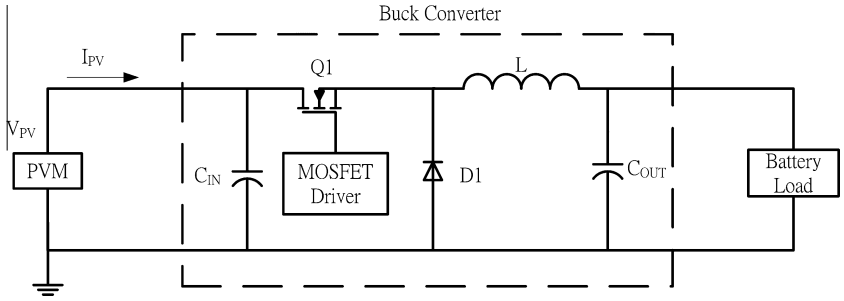

Fig. 3. Standalone PV system with buck-converter design.

Table 2
Parameters used in buck converter simulation.

PV Module	CSSS-90A
V_{BAT}	24 V
V_{FW}	0.7 V
R_{DS}	0.27 Ω
R_L	0.85 Ω

As discussed in Chao et al. (2009) and Pai and Chao, 2010, if the range of variation of D_{MPP} can be estimated, the D_1, D_2, and D_3 should be selected to let D_{MPP} be between D_1 and D_3. For example, if D_{MPP} ranges between 30% and 40%, the D_1, D_2, and D_3 can be 30%, 35%, and 40%. Because D_{MPP} locates between D_1 and D_3, the position can be better estimated by using a quadratic formula. On the other hand, depending on the relative positions of (D_1, P_1), (D_2, P_2), and (D_3, P_3) on the power curve, the QM MPPT introduces three different cases: (a) $P_2 > P_1$ and $P_2 > P_3$; (b) $P_1 > P_2 > P_3$; and (c) $P_3 > P_2 > P_1$.

In case of (a), (D_2, P_2) is the largest power output among the three working points indicating a local maximum exists in the interval of D_1 and D_3. In such a case, the estimated maximum power point can be calculated by a quadratic formula and the smallest power output will be dropped out during the iterative step. It suggests that the remaining points are much closer to the target D_{MPP} after each iterative loop, and it converges to the theoretical MPP effectively.

In the second and third cases, the measured information does not ensure a local maximum value between D_1 and D_3, a duty shifting strategy will be enforced in order to have a convergent tracking result. When P_1 is the largest, it implies that three working duties are in right hand side of MPP, every working duty needs to be shifted to the left by a given step size to guarantee the convergent result. Similarly, all duties are shifted to the right if P_3 is found to be the largest.

If QM MPPT process converges, the algorithm will keep the current D_2 as the estimated D_{MPP}, and compare the output power of the PV array with previous one. If the variation of output power value is larger than a defined value, then the algorithm will restart the MPPT calculation using initial operating points.

However, there are some problems about applying QM method to a PV system on a moving vehicle:

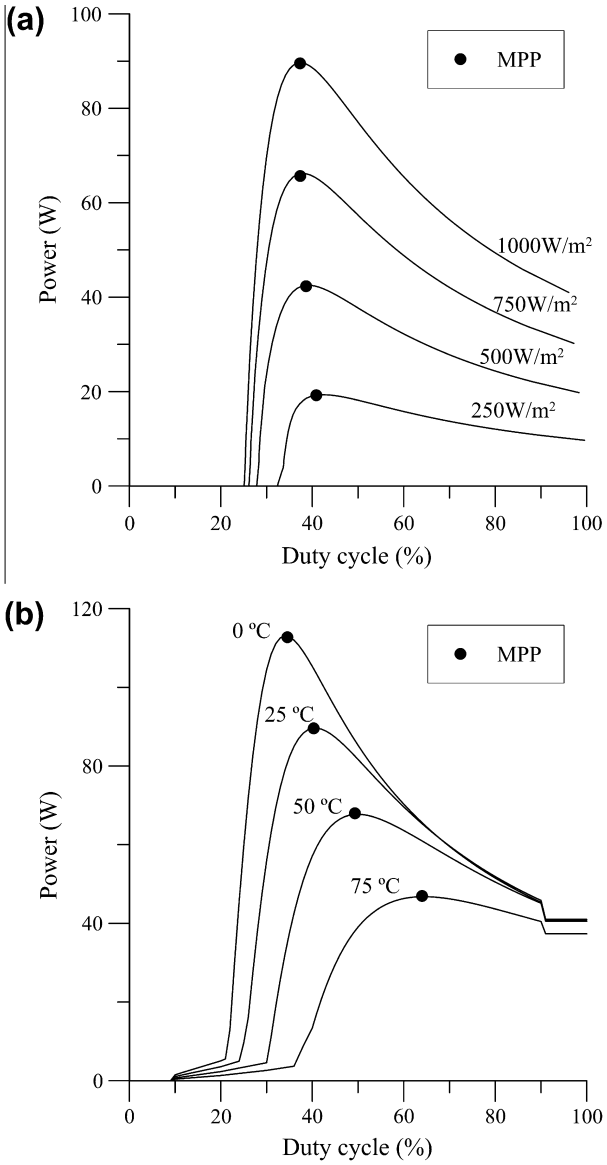

Fig. 4. Power-versus-duty cycle characteristics of the considered PV system: (a) light intensity characteristic at 25 °C; (b) temperature characteristic at 1000 W/m^2.

1) *Duty Shifting*: In the first case of QM MPPT method, the difference between D_1 and D_2, and D_2 and D_3, represented by $\Delta D_1$and ΔD_2 respectively, are

decreased during the process in order to improve the MPPT accuracy. It is possible that case (b) or (c) will happen in the subsequent tracking loop. A smaller ΔD represents a longer track period to find MPP.

2) *Re-tracking*: As described earlier, previous QM method keeps D_2 as final output after reaching the MPP, whereas ΔD_1 and ΔD_2 are getting smaller during the MPPT process. Since smaller ΔD_1 and ΔD_2 are not suitable in the next iteration, it requires reset ΔD_1 and ΔD_2 for restarting MPPT process, and thus causes the unnecessary perturbation to the PV system leading to efficiency drop of the system. The previous QM MPPT experimental result on a model ship is shown in Fig. 5. The model ship stays in dock and rolls slightly. It is found that the D_{MPP} varies only between 48% and 52%, but the unnecessary restart tracking algorithm causes the MOSFET sweeping between 20% and 70% of duty cycle. The efficiency is decreased.

3) *Convergence*: Previously, QM method called a convergent result when the absolute value of power difference in two successive iterations was smaller than a predefined value. When the PV system connected to a resistance type of load, says $R = 1\ \Omega$, it causes a problem. The solid line in Fig. 6 indicates the power characteristic in such a scenario. The curve exhibits a stiff peak of maximum power point. The quadratic formulation curve is illustrated by the dash line. As shown in Fig. 6, the calculated results (D_2 and $D_{2,\mathrm{new}}$) in the two successive iterations are very similar, but still far away from the theoretical MPP. In some situation, the output of QM method is only half of the real maximum power value.

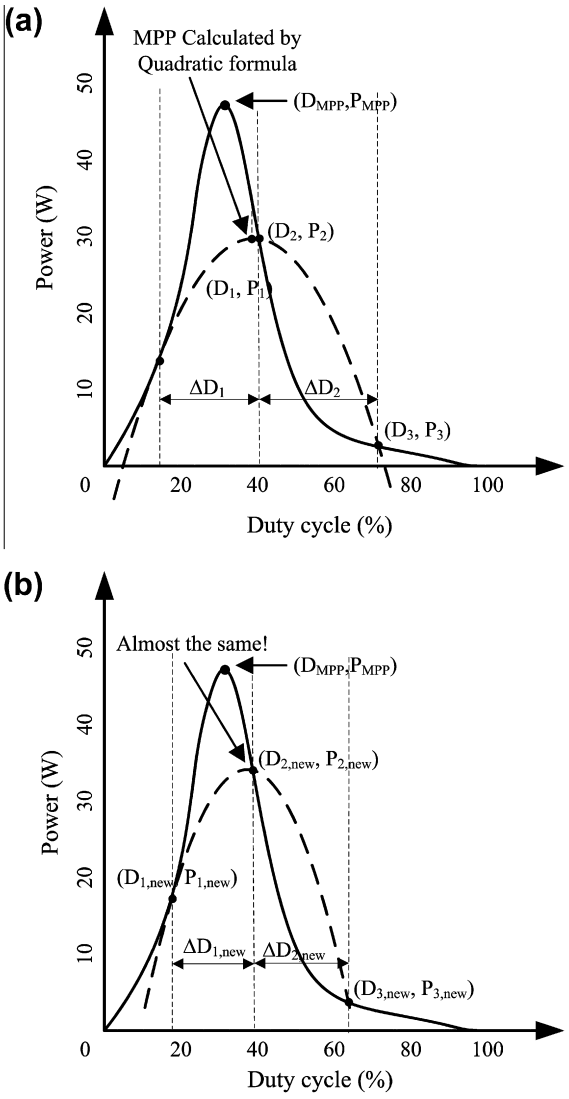

Fig. 6. Illustrative case of failure of quadratic maximization MPPT method applied to a resistance type load: (a) the operating situation at loop #n; (b) at loop #$n+1$, the estimated power is very close to the result at previous loop, but only half of real maximum power is achieved.

3. Modified quadratic maximization method

As discussed in Section 2, the intervals among three operating points are getting smaller during the MPPT process, and it causes the duty shifting and re-tracking problems while applying on a moving vehicle. Moreover, QM method may reach the wrong result in some cases, especially when the PV system is connected to a resistance type of load. To solve this problems, this study proposes a modified quadratic maximization (modified QM) MPPT algorithm.

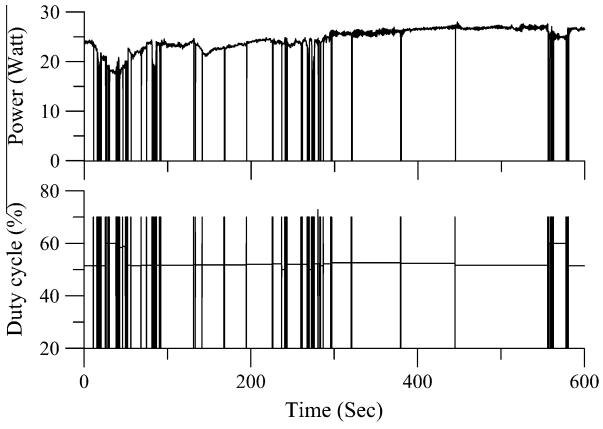

Fig. 5. Use of QM method on a model ship showing un-necessary power and duty fluctuation due to vehicle's dynamic motion.

Firstly, modified QM method uses a dynamic duty step size strategy. Duty step size represents the difference between D_1 and D_2 (ΔD_1), or D_2 and D_3 (ΔD_2). There are three different cases considered in modified QM method similar to the original one. In these cases, in addition to decreasing the duty step size, the proposed method also increases the values of ΔD_1 and ΔD_2.

In the first case, $P_2 > P_1$ and $P_2 > P_3$, a possible operating duty cycle for MPP, D_{est} can be calculated by the quadratic maximization formula

$$D_{est} = \frac{D_1^2 \cdot (P_2 - P_3) + D_2^2 \cdot (P_3 - P_1) + D_3^2 \cdot (P_1 - P_2)}{2[D_1 \cdot (P_2 - P_3) + D_2 \cdot (P_3 - P_1) + D_3 \cdot (P_1 - P_2)]} \tag{5}$$

The estimated duty cycle of MPP is closer to the real D_{MPP} than D_2, and is adopted as the new D_2 in next iteration. Thus the new operating points $D_{1,new}$, $D_{2,new}$, $D_{3,new}$ are determined by

$$\begin{aligned} &D_{2,new} = D_{est};\\ &\Delta D_1 = D_2 - D_1;\\ &\Delta D_2 = D_3 - D_2;\\ &D_{1,new} = D_{2,new} - \alpha\Delta D_1, \text{ where } 0 < \alpha < 1;\\ &D_{3,new} = D_{2,new} - \beta\Delta D_2, \text{ where } 0 < \beta < 1 \end{aligned} \tag{6}$$

In Eq. (6), the $D_{2,new}$ is replaced by previous optimum duty value, D_{est}, and the duty step size ΔD_1 and ΔD_2 are calculated. The new (ΔD_1, ΔD_2) equals the old (ΔD_1, ΔD_2) multiplying a constant (α, β), respectively. The constants α and β range between 0 and 1. The new ΔD_1 and ΔD_2 are getting smaller and smaller during the MPPT process, thus will be convergent to D_{MPP}. If α and β are too large, it will need more time for D_1 and D_3 approaching D_{MPP}, thus reduce the MPPT efficiency. On the other hand, small values of α and β increase the probability of duty shifting, and also reduce the MPPT efficiency. In this study, the values of α and β are determined by trial and error method by using computer simulations.

In the second case, $P_1 > P_2 > P_3$, as shown in Fig. 7, $D_{2,new}$ is replaced by D_1 and $D_{3,new}$ by D_2. The new ΔD_1 equals the old ΔD_2 times a constant γ, and $D_{1,new}$ is the result of $D_{2,new}$ minus the new ΔD_1. Because γ is larger than 1, the duty step sizes ΔD_1 and ΔD_2 are getting larger and larger during the duty shifting process. As a result, this strategy improves the speed of "duty shifting". On the other hand, since ΔD_1 and ΔD_2 are enlarged during the

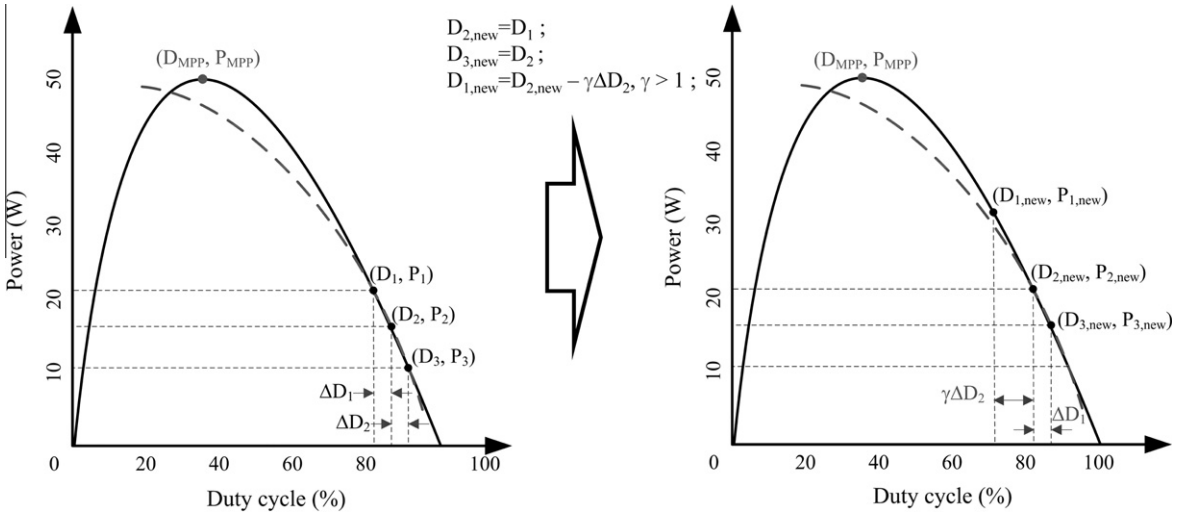

Fig. 7. Dynamic duty adjustment in the proposed algorithm for $P_1 > P_2 > P_3$.

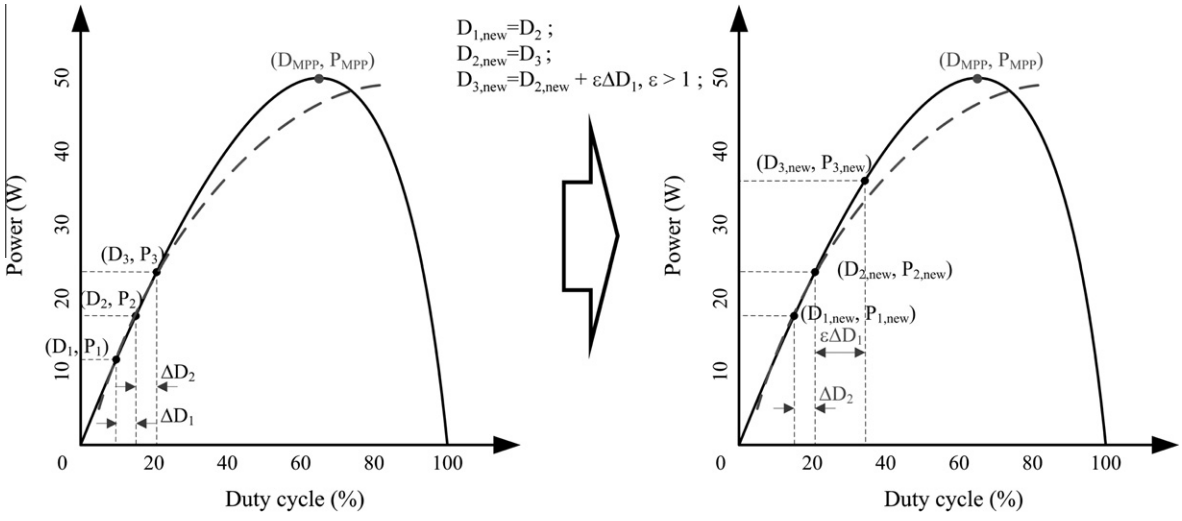

Fig. 8. Dynamic duty adjustment in the proposed algorithm for $P_3 > P_2 > P_1$.

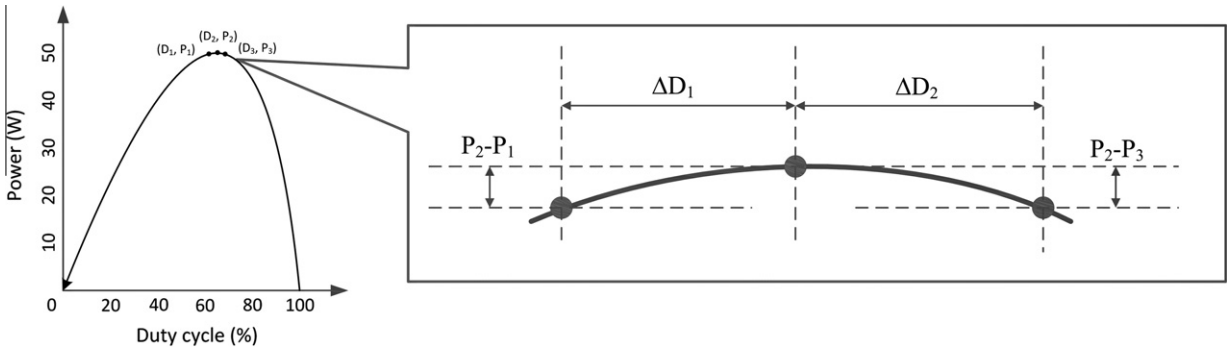

Fig. 9. Illustration of convergent condition of the proposed modified QM method.

MPPT process. There is no need to reset the whole process when MPPT is restarted. Case three when $P_3 > P_2 > P_1$, as shown in Fig. 8, a similar strategy is used.

When the PV system connected to a resistance type of load, it can post a potential problem if the convergent condition is not set properly. That is, the original QM method may track a wrong result, and severely decrease the MPPT efficiency. We propose a normalized convergent condition with respect to the panel rating to cover various panel applications. In the neighborhood of MPP of a power versus duty cycle curve, Fig. 9, the convergent condition of the modified QM method is defined by

$$P_2 > P_1, P_3;\quad \frac{P_2 - P_1}{D_2 - D_1}\frac{1}{P_2} \leqslant \tau;\ \text{and}\ \left|\frac{P_2 - P_3}{D_2 - D_3}\frac{1}{P_2}\right| \leqslant \tau \tag{7}$$

The terms $(P_2–P_1)/(D_2–D_1)$ and $(P_2–P_3)/(D_2–D_3)$ in (7) calculate the slopes between point 1 and point 2, and between point 2 and point 3 respectively. The calculated results are divided by the output power of point 2 to for normalization. Thus the convergent condition is adapted for PV panels of different rating. A convergent result is obtained when the normalized slopes are less than a predefined constant τ. Usually a smaller value of τ produces a more accurate MPPT result, but the range of τ is limited by the accuracy of measurement and the irradiance variation rate. A convergent MPPT result cannot be obtained if τ is not set appropriately.

The flowchart of the proposed QM method is shown in Fig. 10. The algorithm is divided into two stages: data acquisition and MPPT calculation. In data acquisition stage the algorithm first decides the necessary working

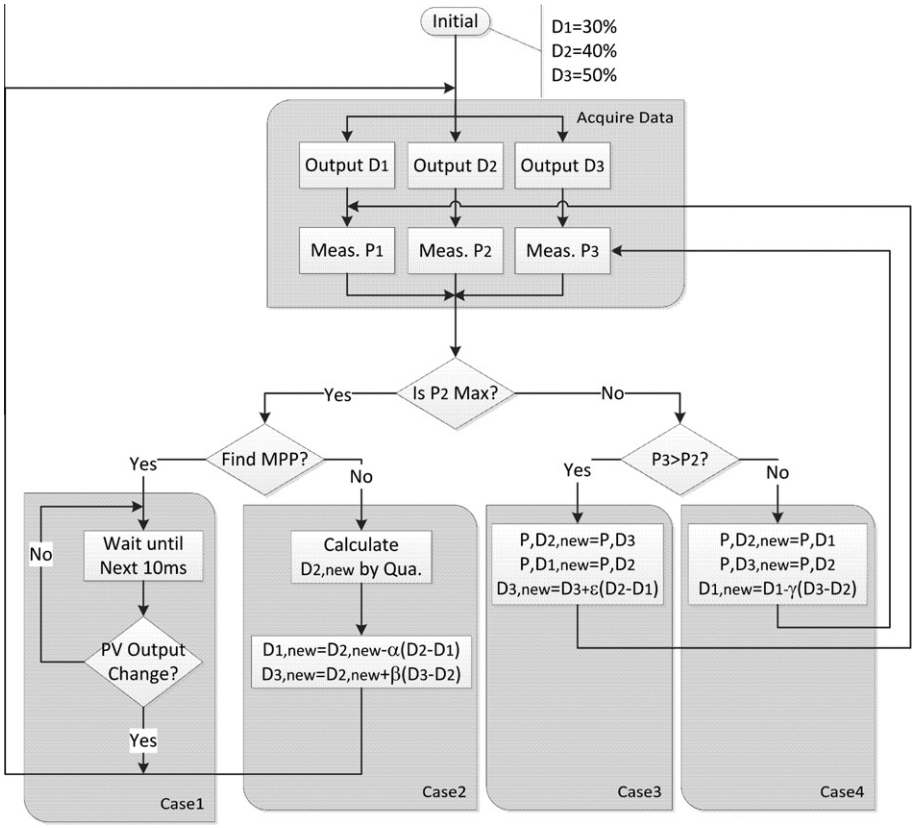

Fig. 10. Modified QM MPPT algorithm flowchart ($\alpha = \beta = 0.625$, $\varepsilon = \gamma = 1.6$, $\tau = 0.02$).

points to be measured, then acquires the power information. According to the relative magnitudes of three operating points, MPPT calculation performs necessary tracking strategies to find the maximum power point of the PV system.

3.1. Benchmark test

To observe the MPPT response to the variation of D_{MPP}, a number of simulations were performed under two different operating conditions: the step change of irradiation and step change of temperature.

For step irradiation change, the irradiation changed suddenly from 500 W/m^2 to 1000 W/m^2 at 390 ms, and followed by 500 W/m^2 at 590 ms. The corresponding D_{MPP} can be found from Fig. 4a. The simulation results are plotted in Fig. 11. In addition to the modified (Fig. 11a) and original QM (Fig. 11b) methods, the conventional P&O result is also illustrated in Fig. 11c. The ΔD used in P&O method was 1%. All MPPT calculation start at 100 ms after system boot up, and the output power and duty cycle are shown on left and right hand side, respectively. From Fig. 4, it is understood that the variation of D_{MPP} due to irradiation change is very limited. When the irradiation changes at 390 ms, the modified QM method spends 20 ms to achieve the MPP, and previous QM method spends 120 ms to complete MPPT. On the other hand, the MPPT efficiency can be evaluated by calculating the energy harvested during the MPPT process. The modified QM method harvests 3.091 mW h, and previous QM method harvests 2.946 mW h. Comparing with the previous QM method, the modified QM method improves about 5% of efficiency. The result shown in Fig. 11c also reveals that at the beginning, the P&O method took about 200 ms to find the MPP, which was obviously longer than the QM method. There is no significant perturbation during the change of irradiation, but there is always a small perturbation even when the MPP was reached.

For step temperature change case, temperature jumping from 0 to 50 °C (at 390 ms), and back to 0 °C (at 590 ms) were discussed. As shown in Fig. 12, both modified and original QM methods immediately reached the convergent results. When the temperature first changed, the performance of modified QM method is slightly better than the previous QM method. When the temperature changed again at 600 ms, because the D_{MPP} is pretty far from the previous D_{MPP}, the modified QM method spend a little more time for duty shifting process, thus seems less efficient than the previous QM method. In fact, the modified and previous QM methods generally have similar responses under the step temperature change. On the other hand,

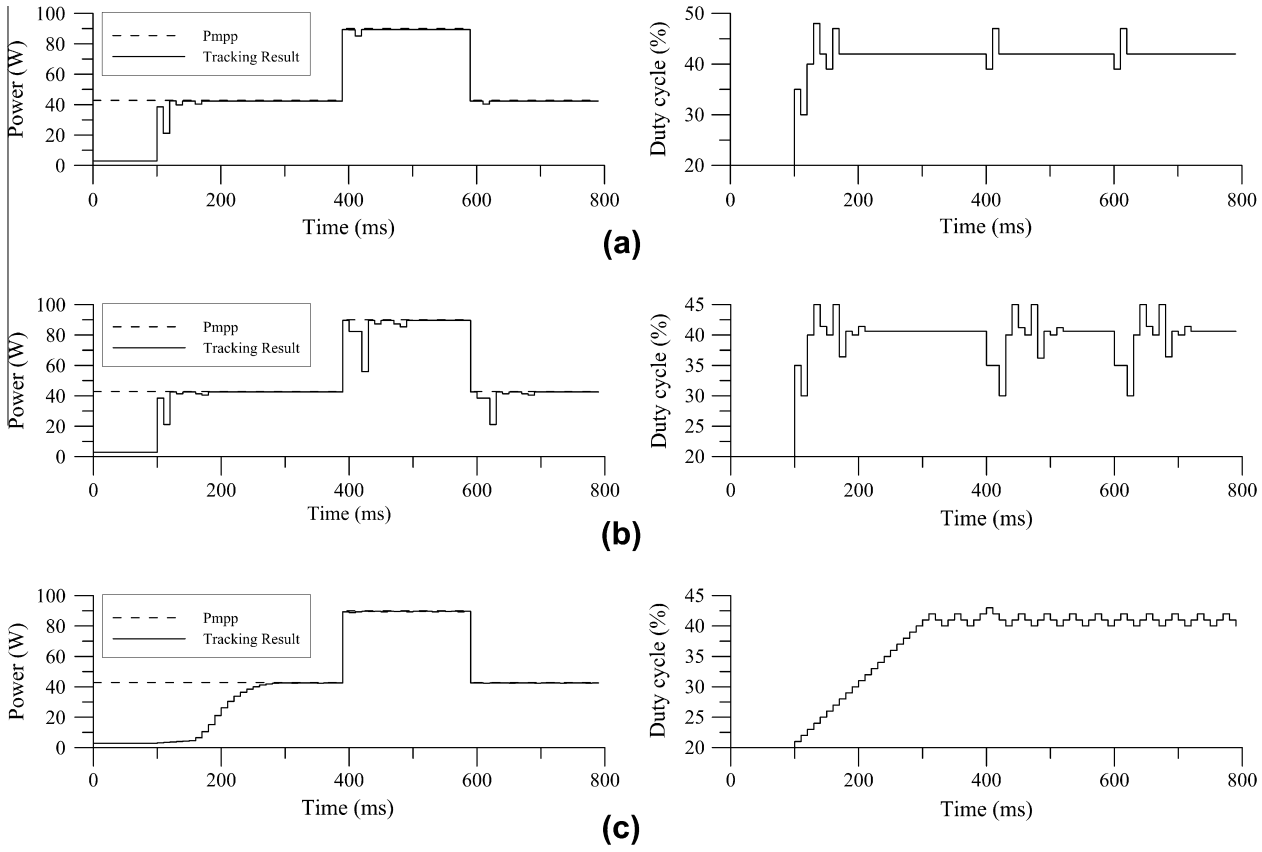

Fig. 11. MPPT results under step changes of insolation (500 W/m^2 → 1000 W/m^2 → 500 W/m^2, temperature = 25 °C): (a) modified QM; (b) original QM; (c) P&O.

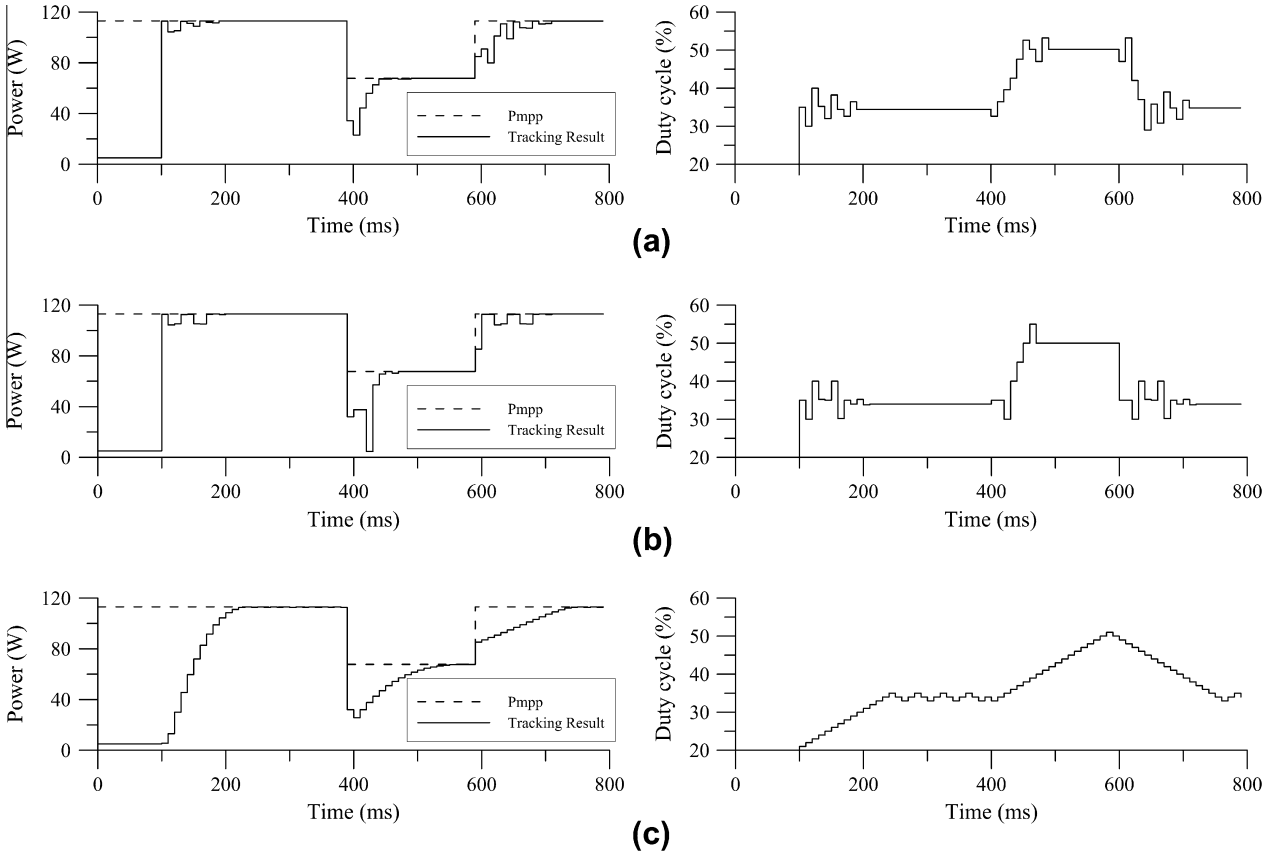

Fig. 12. MPPT results under step changes of temperature (0 °C → 50 °C → 0 °C, radiation = 1000 W/m^2): (a) modified QM; (b) original QM; (c) P&O method.

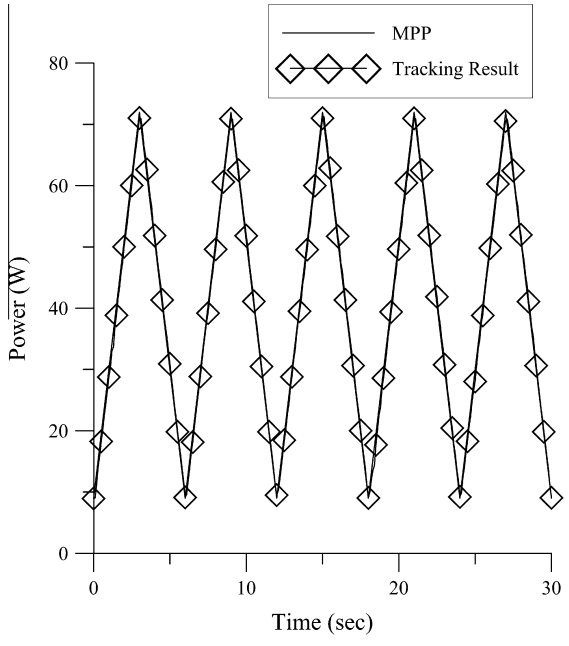

Fig. 13. Fast Ramp MPPT Results (Efficiency = 99.3%), irradiance changes from 200 to 800 W/m^2 (Temperature = 50 °C).

the P&O method, as shown in Fig. 12c, was apparently much slower than the other two methods.

Table 3
Specification of photovoltaic module used on model ship.

Photovoltaic cells	Single crystalline silicon
Voltage at MPP @ STC	16.28 V
Current at MPP @ STC	1.7 A
Short-circuit current @ STC	2.03 A
Open-circuit voltage @ STC	21.65 V

According to the results in Fig. 11, the modified QM method performs great MPPT efficiency over the previous QM method under pure irradiation change. Similar results also can be obtained for small temperature change. The simulation result in Fig. 12 shows that both the modified and previous QM methods have good MPPT performance under rapid temperature change. It is fairly to say that the performance of modified QM method is the best among the methods have been tested, and the proposed method is very appropriate for deploying to a PV system on a moving vehicle.

4. MPPT experiments

4.1. Sandia dynamic performance test (Bower, 2004)

The operation of the modified QM MPPT method has also been evaluated by a simulated dynamic environment.

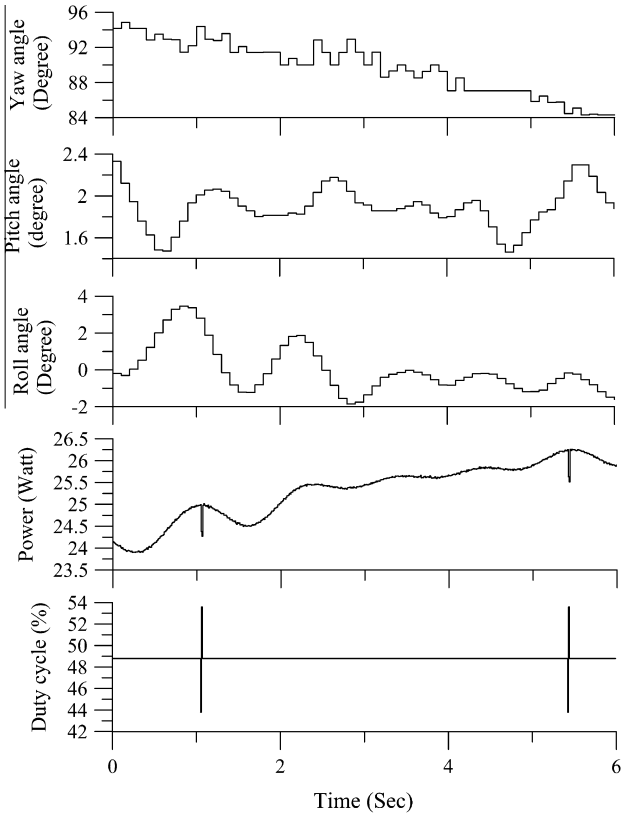

Fig. 14. Example of the dynamic response of the model ship and the power output of the PV system using proposed QM method running on the model ship within 6 s interval, showing minimum duty adjustment.

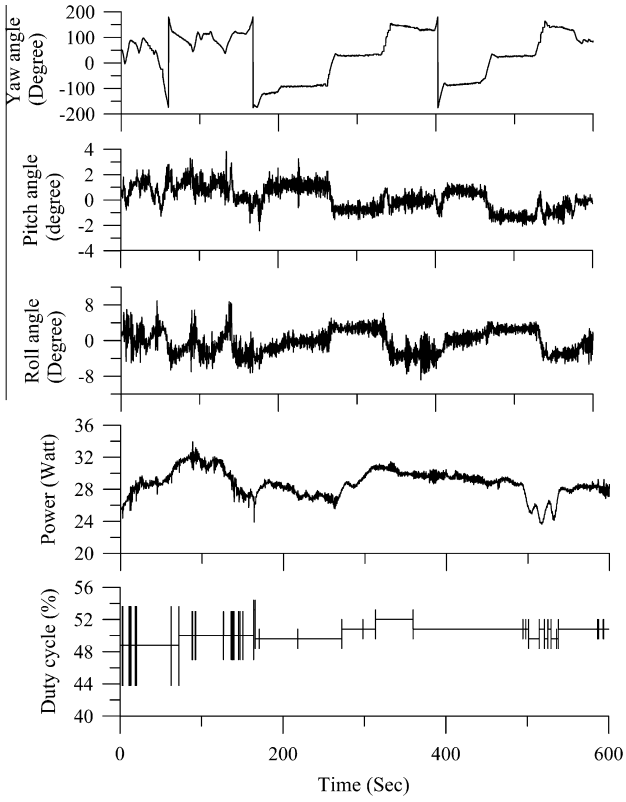

Fig. 15. Dynamic response of the model ship during autonomous operation of the model ship in 10 min, and the power harvesting information and controlled duties during the testing; modified QM method works well with small fluctuation due to vehicle's motion.

A MPPT testing system is established and it follows the protocol suggested by Sandia national laboratories in USA (Bower, 2004). In this experiment, the CSSS-90A PV module is simulated by Agilent E4351B solar array simulator (SAS). The output characteristic of the PV (I_{SC}, I_{MP}, V_{OC}, and V_{MP}) module under different temperature and irradiation was first evaluated by using LabVIEW software according to the MPPT testing protocol of Sandia national laboratories. Then the one-diode model of SAS was used to simulate the output of the PV module. A DC/DC buck converter was designed and tested, and the entire PV system was connected to a 24 V Lead-Acid battery for energy storage. The control and data acquisition system were implemented by a National Instruments™ cRIO controller. The NI 9229 and NI 9227 were used for voltage and current measurements. There were two test procedures adopted in the experiment, including the Fast Ramp and Triangle Ramp procedure.

In the fast ramp experiment, the test began with an irradiance ramp up from 200 to 800 W/m^2 in 3 s ($T = 50$ °C), then ramp down from 800 to 200 W/m^2 in the following 3 s. The procedure was repeated to obtain a total of 5 sets of results. The test determined how quickly the MPPT unit responds to a rapid change in PV output under variation of irradiation. The experimental result is plotted in Fig. 13, and a MPPT efficiency of 99.3% was obtained for the proposed method. That means the modified QM method achieves high efficiency under rapidly change of irradiation.

The triangle ramp test is similar to the fast ramp, but it includes a linear ramp up from 200 to 800 W/m^2 and ramp down to 200 W/m^2 in 60 s. During the test, temperature varies from 0 to 60 °C and back to 0 °C. In the triangle ramp test, the efficiency of the proposed method is 99.4%.

The efficiency of the proposed method is quantified, and high MPPT efficiency values are achieved in both of the fast and the triangle ramp tests. Therefore, the experiments also validated the feasibility of modified QM algorithm in practice.

4.2. Experiment on a model ship

To observe the MPPT performance of the proposed method, an experiment on a model ship was performed in Anping harbor, Tainan, Taiwan. The size of the model ship is about 2-m long, and the ship is equipped with a NI cRIO controller. There are also a GPS module and a inertial measurement unit used for autonomous path tracking purpose. In this experiment, two PV panels connected in series with total 50 W rating are installed, and the specification is shown in Table 3. The model ship followed a rectangular path autonomously.

Fig. 14 shows the PV power output and dynamic information of rolling, pitching and yawing of the solar ship for 6-s interval. The output power of PV system contained a small variation with a frequency near to 1 Hz, which was similar to the pitching and rolling motion of the ship. When the variation was large enough to trigger the re-tracking process of MPPT algorithm (at 1.1 s and 5.3 s), the modified QM method only caused a small perturbation with very short tracking time.

Fig. 15 shows a 10-min autonomous operation of the ship following a rectangular path. Compared with the previous result in Fig. 5, the proposed QM method has less perturbation than the original QM method. For example, the initial values of D_1, D_2, and D_3 used in this experiment are 30%, 35%, and 40%, and it is found that the D_{MPP} varies only between 48% and 52% in this experiment. If the previous QM method is used, the unnecessary restart tracking will cause the MOSFET sweeping between 30% and 55% of duty cycle, thus reduce the efficiency. It is believed that when used with the proposed QM method, the moving ship can always extract maximum power from the sun, and the total efficiency of the PV system is also increased.

5. Conclusion

In this paper, a modified quadratic maximization MPPT algorithm used in the PV system on a moving vehicle is proposed. Firstly, the power generated by the PV system on a moving vehicle is analyzed, and the variation of D_{MPP} under different environment conditions is also discussed. The modified QM method improves the overall tracking efficiency by adopting a new duty shifting strategy and power convergent condition. A dynamic duty adjustment is also employed, which ensures the long term operation of the PV system at its optimum power output condition. The P&O, original and modified QM methods are implemented by LabVIEW and PSIM software for simulation. The simulation results verify the performance of MPPT methods under step and dynamic changes of environment conditions. By using solar array simulator, E4351B, the efficiency of the proposed method is also quantified.

Although the P&O method has a slow restart tracking of the maximum power, its performance is compatible to the modified QM method for insolation changing conditions (Fig. 11a and c). For temperature variation and other testing conditions, the newly proposed QM method outright every method tested during this work and it has the highest maximum power tracking efficiency.

The experiment results by a model ship also show the feasibility of the proposed QM tracking method in a real atmospheric condition. The PV power output is less affected by ship motion of yawing, pitching and rolling, which contributes largely pseudo insolation change. Finally, we also conclude that the proposed method not only can be extended to a PV system with voltage regulator, but also can be used in the development of a distributed PV harvest system in a dynamic changing environment.

Acknowledgments

This research was funded by NSC-100-2221-E-006-019 from the National Science Council, Taiwan, ROC, and is partially supported by RCETS, NCKU.

References

Bose, B.K., Szczesny, P.M., Steigerwald, R.L., 1985. Microcomputer control of a residential photovoltaic power conditioning system. IEEE Transactions on Industry Applications IA-21 (9), 1182–1191.

Bower, W., 2004. Performance test protocol for evaluating inverters used in grid-connected photovoltaic systems. Institute for Sustainable Technology.

Chao, R.M., Lin, I.H., Pai, F.S., Ko, S.H., Chang, C.C., 2009. Evaluation a photovoltaic energy mechatronics system with built in quadratic maximum power point tracking algorithm. Solar Energy 83, 2177–2185.

Erickson, R.W., Maksimović, D., 2001. Fundamental of Power Electronics. Kluwer, Norwell, MA.

Esram, T., Chapman, P.L., 2007. Comparison of photovoltaic array maximum power point tracking techniques. IEEE Transactions on Energy Conversion 22 (2), 439–449.

Femia, N., Petrone, G., Spagnuolo, G., Vitelli, M., 2005. Optimization of perturb and observe maximum power point tracking method. IEEE Transactions on Power Electronics 20 (4), 963–973.

Hussein, K.H., Muta, I., Hshino, T., Osakada, M., 1995. Maximum photovoltaic power tracking: an algorithm for rapidly changing atmospheric conditions. Proceedings of the Institute of Electrical and Electronics Engineers 142 (1), 59–64.

Jain, S., Agarwal, V., 2007. Comparison of the performance of maximum power point tracking schemes applied to signal-stage grid-connected photovoltaic systems. IET Electric Power Applications 1 (5) , 753–762.

Koutroulis, E., Kalaitzakis, K., Voulgaris, N.C., 2001. Development of a microcontrollerbased, photovoltaic maximum power point tracking control system. IEEE Transactions on Power Electronics 16 (1), 46–54.

Liu, F., Duan, S., Liu, F., Liu, B., Kang, Y., 2008. A variable step size INC MPPT method for PV systems. IEEE Transactions on Industrial Electronics 55 (7), 2622–2628.

Pai, F.S., Chao, R.M., 2010. A new algorithm to photovoltaic power point tracking problems with quadratic maximization. IEEE Transactions on Energy Conversion 25 (1), 262–264. http://dx.doi.org/10.1109/TEC.2032575.

Patel, H., Agarwal, V., 2009. MPPT scheme for a PV-fed single-phase single-stage grid-connected inverter operating in CCM with only one current sensor. IEEE Transactions on Energy Conversion 24 (19), 256–263.

Petrone, G., Spagnuolo, G., Teodorescu, R., Veerachary, M., Vitelli, M., 2008. Reliability issues in photovoltaic power processing systems. IEEE Transactions on Industrial Electronics 55 (7), 2569–2580.

Phang, J.C.H., Chan, D.S.H., Phillips, J.R., 1984. Accurate analytical method for the extraction of solar cell model parameters. Electronics Letters 20 (10), 406–408.

Salas, V., Olías, E., Barrado, A., Lázaro, A., 2006. Review of the maximum power point tracking algorithms for stand-alone photovoltaic systems. Solar Energy Materials and Solar Cells 90 (11), 1555–1578.

Xiao, W., Dunford, W.G., Palmer, P.R., Capel, A., 2004. A novel modeling method for photovoltaic cells. In: Proceedings of the. IEEE 35th Annual Power Electron. Spec. Conf. pp. 1950–1956.

Xiao, W., Dunford, W.G., Palmer, P.R., Capel, A., 2007. Regulation of photovoltaic voltage. IEEE Transactions on Industry Electronics 54 (3), 1365–1374.